ELSEVIER

Biophysical Chemistry 109 (2004) 305–324

Biophysical Chemistry

www.elsevier.com/locate/bpc

Reduction of nitrogenase Fe protein from *Azotobacter vinelandii* by dithionite: quantitative and qualitative effects of nucleotides, temperature, pH and reaction buffer

P.E. Wilson, J. Bunker[1], T.J. Lowery[2], G.D. Watt*

Department of Chemistry and Biochemistry, Brigham Young University, Provo, Utah 84604, USA

Received 19 August 2003; received in revised form 3 December 2003; accepted 8 December 2003

Abstract

Oxidized Fe protein from *Azotobacter vinelandii* ($Av2_0$) was reduced by dithionite (DT) in the absence and presence of nucleotides, over the temperature range 10–40 °C, over the pH range 7–8, and in various buffers—inorganic phosphate, TES, HEPES, and Tris. The reduction of each species of Fe protein—$Av2_0$, $Av2_0(MgATP)_2$, and $Av2_0(MgADP)_2$—was resolved into at least three exponential phases, with relative amplitudes of each phase varying over the range of experimental conditions, suggesting a dynamic population shift of kinetically distinct species. The rapid phase of $Av2_0$ reduction predominated at low temperature and pH, and in Tris buffer; rapid $Av2_0(MgATP)_2$ reduction was favored at high temperature and pH, and in phosphate buffer; and $Av2_0(MgADP)_2$ reduction was favored under more physiologically relevant conditions of 20 °C, pH 7.5, and in phosphate buffer. The rates of reduction of Fe protein species did not change with buffer, but temperature and pH do have an effect on the rates. With the appropriate constants, an empirically derived equation estimates the rate of Fe protein reduction at any temperature and pH within the limits 10–40 °C and pH 7–8, for a given species of Fe protein, and a given phase of the reaction. At 23.0 °C and pH 7.4, the rate of the dominant phase of $Av2_0$ reduction is 1.9×10^8 M^{-1} s^{-1}. Under the same conditions, the rates of the two dominant phases of $Av2_0(MgATP)_2$ reduction are 1.2×10^6 and 1.5×10^5 M^{-1} s^{-1}; and the rate of the dominant phase of $Av2_0(MgADP)_2$ reduction is 3.5×10^6 in M^{-1} s^{-1}. Thermodynamic activation parameters for each phase of reduction were calculated. No breaks in the Arrhenius plots for any Fe protein species were observed.

Keywords: Nitrogenase kinetics; Stopped-flow spectroscopy; Arrhenius plot

Abbreviations: $Av2_n$–Fe protein from *Azotobacter vinelandii*, with *n* corresponding to the level of reduction of the [4Fe–4S] cluster—an analogous notation of E_n for MoFe protein in the Thorneley-Lowe model. So $Av2_0$ is in an oxidized $[4Fe–4S]^{2+}$ state; $Av2_1$ is in a reduced $[4Fe–4S]^{1+}$; $Av2_2$ is in an all-ferrous $[4Fe–4S]^0$ state; HEPES–*N*-2-hydroxyethylpiperazine-*N*-2-ethanesulfonic acid; TES–*N*-tris[hydroxymethyl]methyl-2-aminoethanesulfonic acid; Tris–tris (hydroxymethyl) aminomethane.

*Corresponding author. Tel.: +1-801-4224561; fax: +1-801-4225474.

E-mail address: gdw4@email.byu.edu (G.D. Watt).

[1] Brigham Young University Undergraduate Research Program.

[2] Brigham Young University Undergraduate Research Program.

0301-4622/04/$ - see front matter © 2003 Elsevier B.V. All rights reserved.
doi:10.1016/j.bpc.2003.12.002

1. Introduction

Biological nitrogen fixation is the conversion of N_2 into NH_3 by the nitrogenase enzyme, consisting of the redox-active Fe and MoFe proteins. The Fe protein is reduced and binds two MgATP to become the specific reductant to the MoFe protein. Formation of a transient complex between the Fe and MoFe proteins induces ATP hydrolysis and inter-protein electron transfer. The MoFe protein contains the FeMo cofactor, where electrons accumulate and where substrates (e.g. N_2 and H^+) bind for eventual reduction.

The reduction of oxidized Fe protein in the presence and absence of nucleotides and the relative binding strengths of nucleotides to both the oxidized and reduced forms of the Fe protein have been important areas of study in attempts to understand how Fe protein reduction, nucleotide binding, electron transfer, and nucleotide hydrolysis influence nitrogenase catalysis [1–6]. This is the first attempt to characterize Fe protein reduction over a broad set of conditions of temperature, pH and buffers.

2. Theory

Two important reactions describe the reduction of Fe protein by dithionite [2] [7]:

$$DT \underset{k_{DT}}{\overset{k_{-DT}}{\rightleftarrows}} 2\,SO_2^-, \tag{1}$$

where DT is dithionite, $S_2O_4^{2-}$, and

$$SO_2^- + OH^- + Av2_0 \overset{k_r}{\rightarrow} HSO_3^- + Av2_1, \tag{2}$$

where the terms $Av2_0$ and $Av2_1$ are oxidized ($[4Fe–4S]^{2+}$) and reduced ($[4Fe–4S]^{1+}$) forms of Fe protein from *Azotobacter vinelandii*, respectively. The $Av2_0$ term in Eq. (2) refers to any of the oxidized forms of the Fe protein, namely free $Av2_0$, $Av2_0(MgATP)_2$ or $Av2_0(MgADP)_2$, with corresponding reduction rates $k_{r,\ free}$, $k_{r,\ ATP}$ or $k_{r,\ ADP}$.

An analysis of the differential equations describing Eqs. (1) and (2) yields two useful limiting cases. The first of these cases is where $k_r\,[Av2_0] \gg 2\,k_{-DT}\,[SO_2^-]$. This condition applies particularly to reduction of $Av2_0$, whose k_r is fast, and the following equation can be used:

$$[Av2_0] = [Av2_0]_0 - 2\,k_{-DT}\,[DT]\,t. \tag{3}$$

This linear equation applies for early t, until $[Av2_0]$ decreases enough that the first limiting case no longer applies. To relate Eq. (3) to the measured drop in absorbance, we start with the relationship:

$$\Delta Abs = \varepsilon_0\,\Delta[Av2_0]\,l + \varepsilon_1\,\Delta[Av2_1]\,l, \tag{4}$$

where the change in absorbance, ΔAbs, depends on the change in concentrations of $Av2_0$ and $Av2_1$, on their respective extinction coefficients, $\varepsilon_0 = 17.5$ and $\varepsilon_1 = 11.5\ mM^{-1}\ cm^{-1}$ at 400 nm [8], and on the path-length of the stopped-flow apparatus ($l = 1$ cm). The change in [DT] is assumed negligible. For every $Av2_0$ reduced, an $Av2_1$ is formed, so Eq. (4) becomes,

$$\begin{aligned}\Delta Abs &= \varepsilon_0\,\Delta[Av2_0]\,l - \varepsilon_1\,\Delta[Av2_0]\,l \\ &= (\varepsilon_0 - \varepsilon_1)\,\Delta[Av2_0]\,l.\end{aligned} \tag{5}$$

Combining Eqs. (3) and (5), we obtain the relationship:

$$k_{-DT} = \frac{m}{2[DT](\varepsilon_1 - \varepsilon_0)l}. \tag{6}$$

The second limiting case of the differential equations describing Eqs. (1) and (2) occurs when $2\,k_{-DT}\,[SO_2^-] \gg k_r\,[Av2_0]$, and applies at higher t to stopped-flow time courses that initially have a linear portion. For time courses lacking an initial linear portion, this second limiting case is true for all t. The consequence is that $[Av2_0]$ decays exponentially according to the equation:

$$[Av2_0] = [Av2_0]_0 e^{\left(-k_r\sqrt{K_{DT}[DT]}t\right)}, \tag{7}$$

where $K_{DT} = k_{-DT}/k_{DT}$. The observed rate constant of exponential decay is, therefore equal to $k_r\,K_{DT}^{1/2}[DT]^{1/2}$. If [DT] is known, it is easy to calculate an adjusted rate constant, $k_r\,K_{DT}^{1/2}$, so that

samples reduced at different [DT] can be compared.

3. Materials and methods

3.1. Solutions and proteins

Nitrogenase Fe protein from *A. vinelandii* (Av2) with specific activities between 1800–2000 nmol of H_2 mg^{-1} min^{-1} was isolated, purified and characterized as described [9]. All sample preparation, solution transfers and size exclusion chromatography were conducted in a Vacuum Atmospheres glove box under nitrogen at oxygen levels below 1.00 ppm (Nyad O_2-Monitor). All UV-Visible spectra were recorded on a Hewlett Packard 8453 UV Spectrophotometer, located inside the glove box. Oxidized Av2 ($Av2_0$) concentrations were determined by absorbance at 400 nm ($\varepsilon_{400}=17.5$ mM^{-1} cm^{-1}) [8]. [10].

Stock $Av2_1$ was oxidized with excess methylene blue and subsequently separated using anaerobic G-50 Sephadex column chromatography. After separation, the $Av2_0$ optical spectrum was recorded to ensure complete separation from the methylene blue and to determine protein concentration. Dithionite solutions were made inside the glove box and were standardized by absorbance at 315 nm ($\varepsilon_{315}=8.1$ mM^{-1} cm^{-1}) [11].

3.2. Stopped-flow instrumentation

Stopped flow measurements were conducted using an Applied Photophysics Sequential SX-18MV Stopped-Flow Reaction Analyzer connected to a Neslab RTE-111 Refrigerated Bath/Circulator. The sample-handling unit of the stopped-flow was contained inside the glove box. Reduction of the Fe protein was monitored at either 400 or 430 nm using the one-centimeter path length. Av2 concentrations for all runs were known to within ± 3 μM, and all temperatures were known to within ± 0.1 °C. All concentrations reported are the concentrations in the reaction cell after mixing. All reaction progress curves accounted for the complete reduction of all $Av2_0$ present within our experimental error. All reactions were conducted in 50 mM buffers: inorganic phosphate, TES, Tris or HEPES. Progress curves were obtained in the stopped-flow for the reduction of $Av2_0$, $Av2_0(MgATP)_2$ and $Av2_0(MgADP)_2$ by averaging at least three consecutive runs under various conditions of pH 7.0–8.0 and temperature 10.0–40.0 °C. Samples with nucleotides had protein, magnesium, and nucleotides together in the same syringe prior to protein reduction.

3.3. Data analysis

Some kinetic traces were fit to an initial linear portion, and all traces were fit to an equation of the form:

$$\mathrm{Abs}(t)=A_1\ \mathrm{e}^{-k_1 t}+A_2\ e^{-k_2 t}+\cdots+A_n\ \mathrm{e}^{-k_n t} + A_{n+1}, \tag{8}$$

where $\mathrm{Abs}(t)$ is the absorbance as a function of time, with contributions from different exponential terms with apparent rate constants, k_n, and amplitudes, A_n.

Adjusted rate constants $k_{-\mathrm{DT}}$ and $k_{\mathrm{r}}\ K_{\mathrm{DT}}^{1/2}$ were calculated from Eqs. (6) and (7), respectively. The activation energy of a reaction was obtained from the best-fit line of $\ln(k)$ vs. $1000/T$, according to the Arrhenius equation:

$$k=A\mathrm{e}^{(-E_a/RT)}$$
$$\ln(k)=-\frac{E_a}{R}\left(\frac{1}{T}\right)+\ln(A), \tag{9}$$

where k is the adjusted rate constant (either $k_{-\mathrm{DT}}$ or $k_{\mathrm{r}}\ K_{\mathrm{DT}}^{1/2}$), E_a is the energy of activation, R is the gas constant (8.314 J/mol K), T is the temperature in Kelvin, and A is the pre-exponential factor. The activation energy, E_a, is calculated as $-R$ times the slope of the line to yield units in kJ/mol.

In a similar fashion, the activation enthalpy and entropy of a reaction was obtained by fitting the data to the Eyring equation:

$$\ln\left(\frac{kh}{k_{\mathrm{B}}T}\right)=-\frac{\Delta H^{\ddagger}}{R}\left(\frac{1}{T}\right)+\frac{\Delta S^{\ddagger}}{R}, \tag{10}$$

where k, T and R are as before in Eq. (9), and

where h is Planck's constant (6.626×10^{-34} J s), k_B is Boltzmann's constant (1.380×10^{-23} J/K), $\Delta H^{\ddagger}$ is the activation enthalpy in kJ/mol (when plotting vs. $1000/T$), and $\Delta S^{\ddagger}$ is the activation entropy in J/K mol.

For better qualitative comparison of kinetic traces shown in figures, the data has been modified to account for variations in protein concentrations between samples according to the equation:

Relative Reaction Progress

$$= \frac{\mathrm{Abs}(t) - \mathrm{Abs}_{\min}}{\mathrm{Abs}_{\max} - \mathrm{Abs}_{\min}}, \quad (11)$$

where $\mathrm{Abs}(t)$ is the absorbance at a give time, and $\mathrm{Abs}_{\min}$ and $\mathrm{Abs}_{\max}$ are the minimum and maximum absorbance values over the course of a kinetic trace, respectively. This modification facilitates a qualitative comparison of traces at different temperatures and pH values because all traces cross the y-axis at 1.0 and reach the x-axis at the same time. For comparison of traces where the resolution of data points was different at early t, and where the end times were different, care was taken to apply Eq. (11) at coincident t from one trace to another from start to finish of data manipulation.

4. Results

4.1. Reduction of $Av2_0$ by DT

The reduction of free $Ac2_0$ consists of several distinct kinetic phases whose time constants range from milliseconds to over 10 s [2]. We also report that the reduction of $Av2_0$ consists of several distinct kinetic phases. Specifically, over the entire range of conditions from 10–40 °C and pH 7–8, the raw data were fit to three exponential terms, i.e. up to $n=3$ in Eq. (8).

Representative data for the reduction of $Av2_0$ as a function of temperature in phosphate buffer are shown in Fig. 1. Fast and slow phases of the reaction are evident. The fast phase of each kinetic trace is completed within the first 0.2 s for all temperatures shown, and appears superimposed on the y-axis in the figure. Interestingly, the amplitude of the fast phase diminishes with increasing temperature, as should be clear by where the kinetic traces appear to leave the y-axis. The rate of $Av2_0$ reduction in all three phases is faster with increasing temperature.

The effect of pH on the reaction also shows a consistent trend at any given temperature over the range of 10–40 °C. Representative kinetic traces are shown in Fig. 2 for this effect at ~30 °C. The rate of reduction for each exponential term decreases slightly with increasing pH, and the amplitude of the fast reaction decreases with increasing pH.

While the comparison of traces in Figs. 1 and 2 is largely qualitative, a more rigorous analysis of temperature and pH effects was performed. After correcting observed rate constants for small variation in the DT concentration, the raw data were further analyzed by Eq. (8) to yield best-fit apparent rate constants and amplitudes of exponential terms. Arrhenius plots of the fast reaction (data not shown) at constant pH show that the activation energy varies only slightly from one pH value to another. Table 1 summarizes the averages for the activation parameters—E_a, $\Delta H^{\ddagger}$, and $\Delta S^{\ddagger}$—for each phase of $Av2_0$ reduction.

The effects of pH and temperature on $k_{r,\,\mathrm{free},\,1}\,K_{DT}^{1/2}$ (the adjusted rate of reduction of free $Av2_0$ in the fast phase, $n=1$ in Eq. (8)) are shown in Fig. 3. Note that the rate varies essentially linearly with pH, and that this pH effect is more pronounced at high temperatures. For a given temperature but varying pH, linear least-squares fits of the data yield lines (not shown) with increasingly negative slopes (m) and higher intercepts (s) that follow a predictable pattern. A plot of $\ln(-m)$ vs. $1/T$ fits to a straight line with slope $-a$ and intercept b; and a plot of $\ln(s)$ vs. $1/T$ fits to a straight line with slope $-c$ and intercept b. Working backwards, one can derive the relationship:

$$k_r K_{DT}^{1/2} = -e^{[a/T+b]}\mathrm{pH} + e^{[c/T+d]}, \quad (12)$$

where T is in Kelvin. The values of a, b, c and d for each phase of the reduction of $Av2_0$ are given in Table 1. For comparison of rate constants measured in different buffers, we accounted for a temperature-dependent pH change, where the

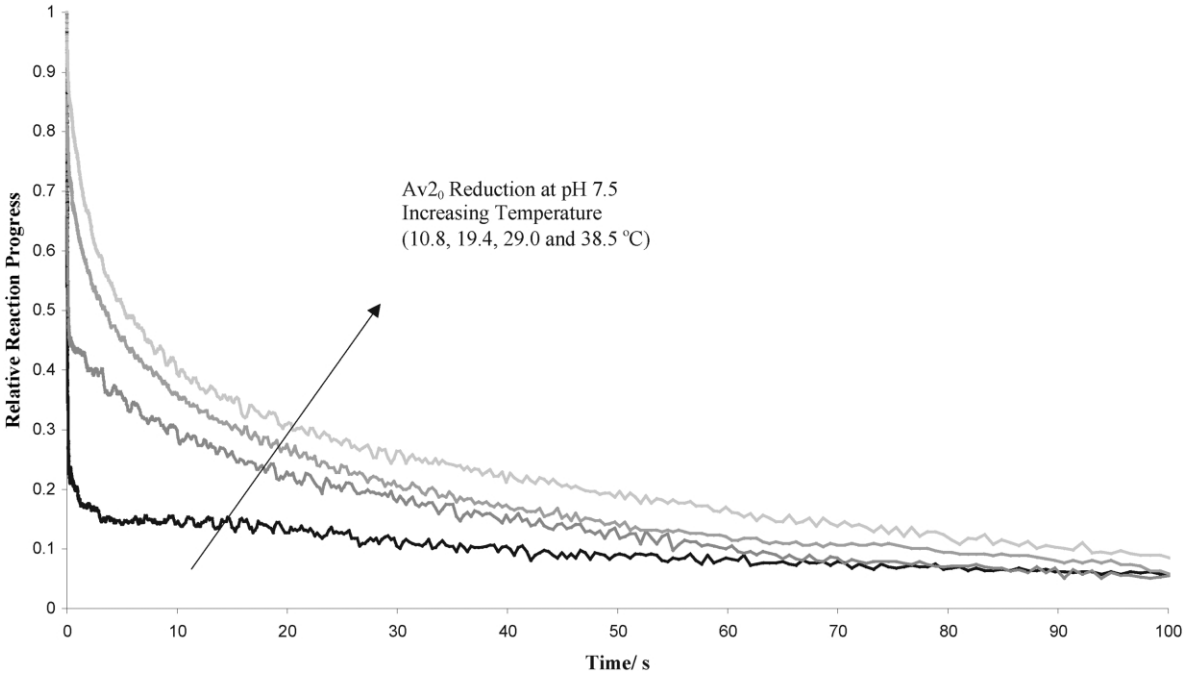

Fig. 1. The reduction of 20 ± 3 μM, free Av2$_0$ by 0.25 mM DT at 10.8, 19.4, 29.0, and 38.5 °C; and pH held constant at 7.5 in 50 mM inorganic phosphate buffer. The data shown are representative of the temperature effect on Av2$_0$ reduction at all pH values studied, and have been modified according to Eq. (11) to facilitate a qualitative comparison.

$\Delta pK_a/°C$ is -0.020 in TES, -0.014 in HEPES, and -0.031 in Tris [12]. The $\Delta pK_a/°C$ for phosphate buffer is negligible.

The procedure used to derive Eq. (12) is useful for estimating the values of *a*, *b*, *c* and *d*; but a global fit of Eq. (12) on the original data yields a more accurate determination of these constants, along with standard errors. The fitting method implemented in Fig. 3 uses weighted non-linear least squares in Microsoft Excel [13]. The straight lines in Fig. 3 represent a simplified form of this data fit, assuming a constant temperature for each line (the average temperature for data points in a given general temperature range). Therefore the actual fit of the data is better than that portrayed because it accounts for subtle temperature and pH variations. However, a significant trend in Fig. 3 is the apparent worsening of the fit to the data with increasing temperature. This is a consequence of weighting the fit according to the reciprocal of the square of the standard deviation [13]. The standard deviation of rate constants within a general temperature range generally increases with temperature. For the 14.8 and 24.9 °C subsets of data points at relatively constant temperature and pH, the standard deviation was taken to be the standard deviation of the rate constants. For the other data subsets that span a larger pH range, we determined the standard deviation from a linear fit with pH. In each case of assessing standard deviation, we ignored temperature variation within data subsets.

The amplitudes of the different phases of Av2$_0$ reduction that accompany fits of [Eq. (8)] to data did not follow as predictable a trend with temperature and pH as the rate constants of the different phases. Still, the results using Eq. (8) are in harmony with the qualitative behavior of kinetic traces in Figs. 1 and 2, as shown in Fig. 4. The relative amplitude of the fast reaction, A_1 (see Eq. (8)), decreases with temperature and pH. Furthermore, the slowest phase, A_3, is responsible for the

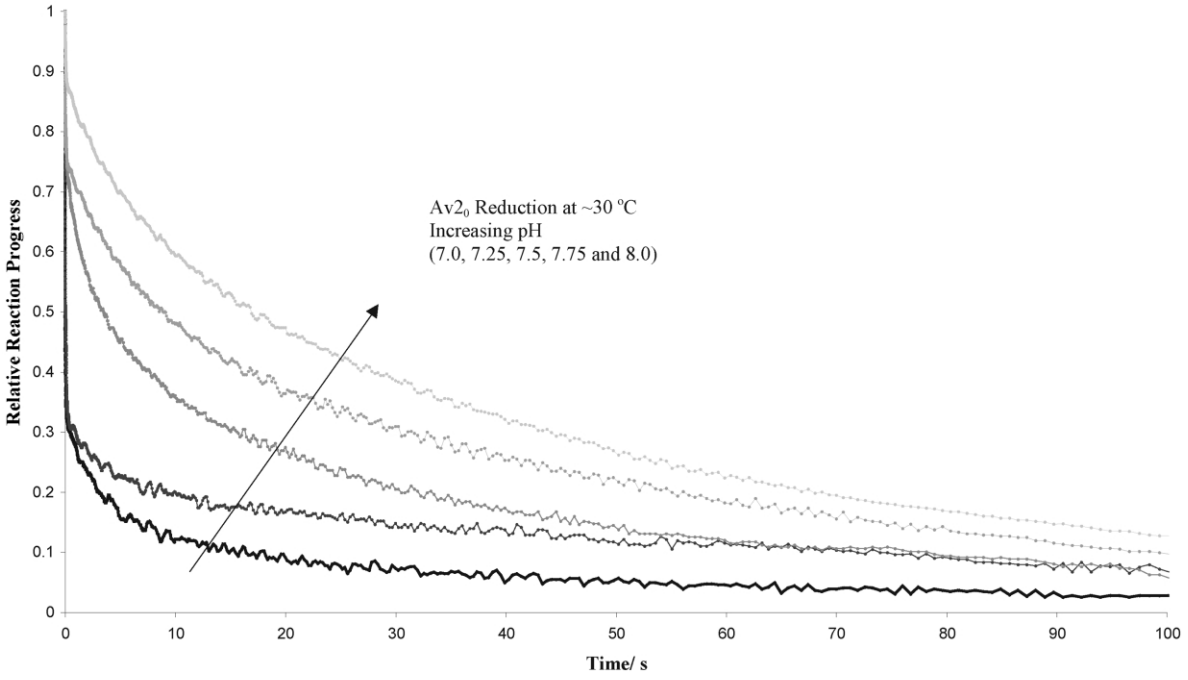

Fig. 2. The reduction of 20 ± 3 μM, free $Av2_0$ by 0.25 mM DT at pH 7.0, 7.25, 7.5, 7.75, and 8.0 in 50 mM inorganic phosphate buffer; and temperature held constant at 29.4 ± 0.6 °C. The data shown are representative of the pH effect on $Av2_0$ reduction at all temperatures studied, and have been modified according to Eq. (11) to facilitate a qualitative comparison.

majority of the compensatory $Av2_0$ reduction with the loss of A_1, while A_2 remains relatively constant at only approximately 10% of the total absorbance change. With declining amplitude at high temperatures and with a rate approaching the dead time of the stopped-flow apparatus, it was difficult to

Table 1
Thermodynamic activation parameters and constants given to estimate the value of $k_{r,\ n}\ DT^{1/2}$ for the reduction of Fe protein species—$Av2_0$, $Av2_0(MgATP)_2$, and $Av2_0(MgADP)_2$—in different exponential phases $n = 1$, 2, etc., in order of decreasing rate. The constants *a*, *b*, *c* and *d* are generally applicable to Eq. (12) over the temperature range 10–40 °C and pH 7–8. Phases that predict traditionally accepted reaction rates at ~23 °C and pH 7.4 are bolded for emphasis. Compare with Table 2

	n	E_a/ kcal/mol	$\Delta H^{\ddagger}$/ kJ/mol	$\Delta S^{\ddagger}$/ J/K mol	$k_r K_{DT}^{1/2} = -e^{\lvert -a/T + b \rvert} pH + e^{\lvert -c/T + d \rvert}$			
					a	*b*	*c*	*d*
Free	**1**	**20.1 ± 0.9**	**82 ± 4**	**105 ± 12**	**7650.171 ± 0.010**	**33.61 ± 0.18**	**8172.451 ± 0.039**	**37.72 ± 0.13**
	2	11.8 ± 1.8	47 ± 8	−76 ± 26			5960 ± 930	21.4 ± 3.1
	3	6.2 ± 1.5	24 ± 6	−201 ± 21	4700.015 ± 0.037	11.12 ± 0.26	4339.982 ± 0.042	12.12 ± 0.21
MgATP	1	−0.4 ± 1.2	−4 ± 5	−204 ± 17			−124 ± 660	6.2 ± 2.2
	2	**2.2 ± 1.2**	**7 ± 5**	**−192 ± 18**			**1130 ± 620**	**7.4 ± 2.1**
	3	**12.4 ± 1.5**	**49 ± 6**	**−64 ± 22**	**11 523.5437 ± 0.0022**	**39.29 ± 0.17**	**9919.7485 ± 0.0066**	**36.31 ± 0.14**
	4	14.7 ± 1.3	59 ± 5	−48 ± 18			7390 ± 640	24.7 ± 2.1
MgADP	1	12.9 ± 5.1	52 ± 21	4 ± 74			6500 ± 2600	30.9 ± 8.9
	2	**23.4 ± 0.8**	**96 ± 3**	**119 ± 11**	**10 223.89 ± 0.13**	**37.89 ± 0.30**	**10 577.35 ± 0.14**	**41.57 ± 0.19**
	3	11.7 ± 3.0	47 ± 13	−78 ± 42	11 772.699 ± 0.095	40.95 ± 0.91	11 445.608 ± 0.087	42.05 ± 0.78

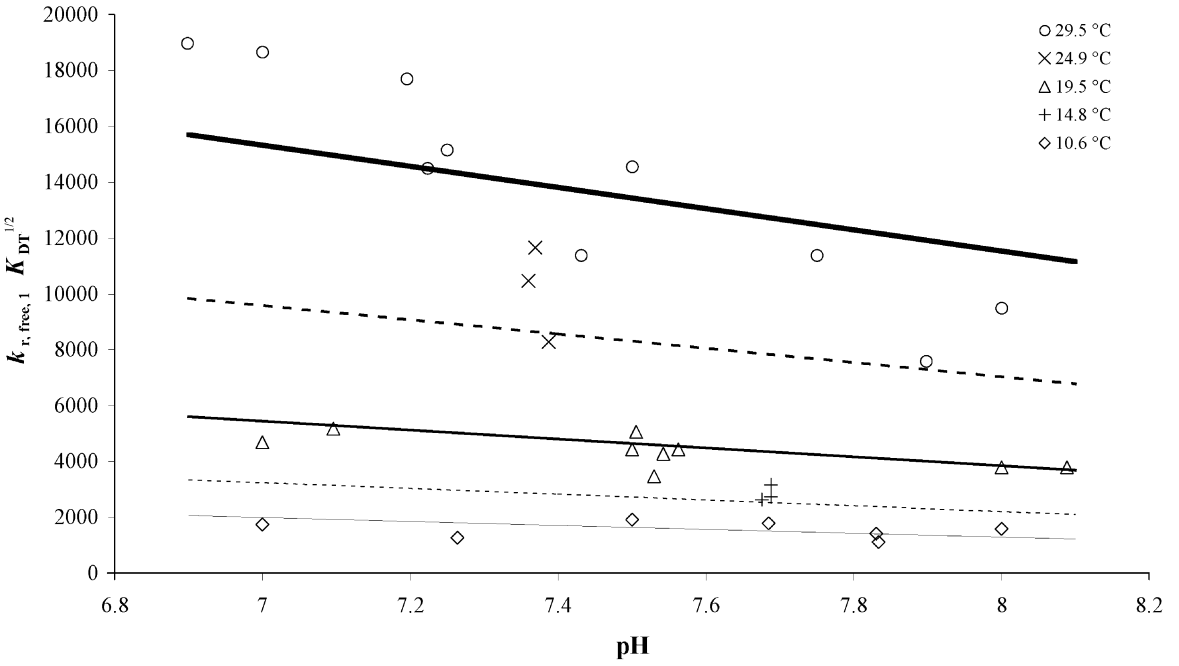

Fig. 3. Effects of pH and temperature on the phase-1 rate constant for $Av2_0$ reduction, $k_{r,\ free,\ 1}\ ^{1/2}_{DT}$, and fit to Eq. (12) (straight lines). Survey of data from reduction of 20 ± 3 μM free $Av2_0$ by 0.25 mM DT in inorganic phosphate, TES, HEPES and Tris buffers over the temperature range ~10–40 °C and pH ~7.0–8.0. Average temperatures for the data within a general temperature range are 10.6 ± 0.5, 14.8 ± 0.2, 19.5 ± 0.5, 24.9 ± 0.5 and 29.5 ± 0.7 °C.

accurately measure $k_{r,\ free,\ 1}\ K_{DT}^{1/2}$ above 30 °C. Still, the phase-1 constants in Table 1 are consistent with the data up to 40 °C. The pH effect for phase 2 was too minor to justify assigning constants for it, possibly because of difficulties in measuring the rate of a phase of such low amplitude. In this case, the pH term in Eq. (12) drops out, leaving only constants *c* and *d* in Table 1 for an alternate form of the Arrhenius equation [see Eq. (9)].

While the analysis in this study has focused on the effects of pH and temperature on the exponential portions of $Av2_0$ reduction, a brief look at the linear portion predicted by Eq. (3) is in order. This equation is only valid for the condition $k_r\ [Av2_0] \gg 2\ k_{-DT}\ [SO_2^-]$, which is applicable to phase-1 reduction especially at low pH. There is sufficient reduction in the fast phase in phosphate buffer to accurately measure the activation energy of k_{-DT} at pH 7.0 to be 24 ± 5 kcal/mol, in agreement with the value of 24.1 kcal/mol determined previously by Lambeth and Palmer at pH 8.0 [7]. One may infer that the rate of monomerization of DT [Eq. (1)] is pH-independent because of this agreement. Unfortunately, k_{-DT} measured from the linear portion above pH 7.0 was significantly slower than expected, progressively worsening with increasing pH. This should be attributed to a DT-independent mechanism. There is likely a breakdown in the condition $k_r\ [Av2_0] \gg 2\ k_{-DT}\ [SO_2^-]$ because it is only true for large $k_r\ [Av2_0]$. As the amplitude of the fast reaction decreases at higher temperatures and pH values, phases with slower k_r predominate. Thus for temperatures above 30 °C and pH above 7, what may appear as a linear portion (usually very short) should be accounted as an hybrid between a line and an exponential that could only be fit accurately to the complete set of differential equations describing Eqs. (1) and (2). This is because experimental conditions present an intermediate state between the assumption used to derive Eq. (3) and the assumption used to derive Eq. (7). The less rig-

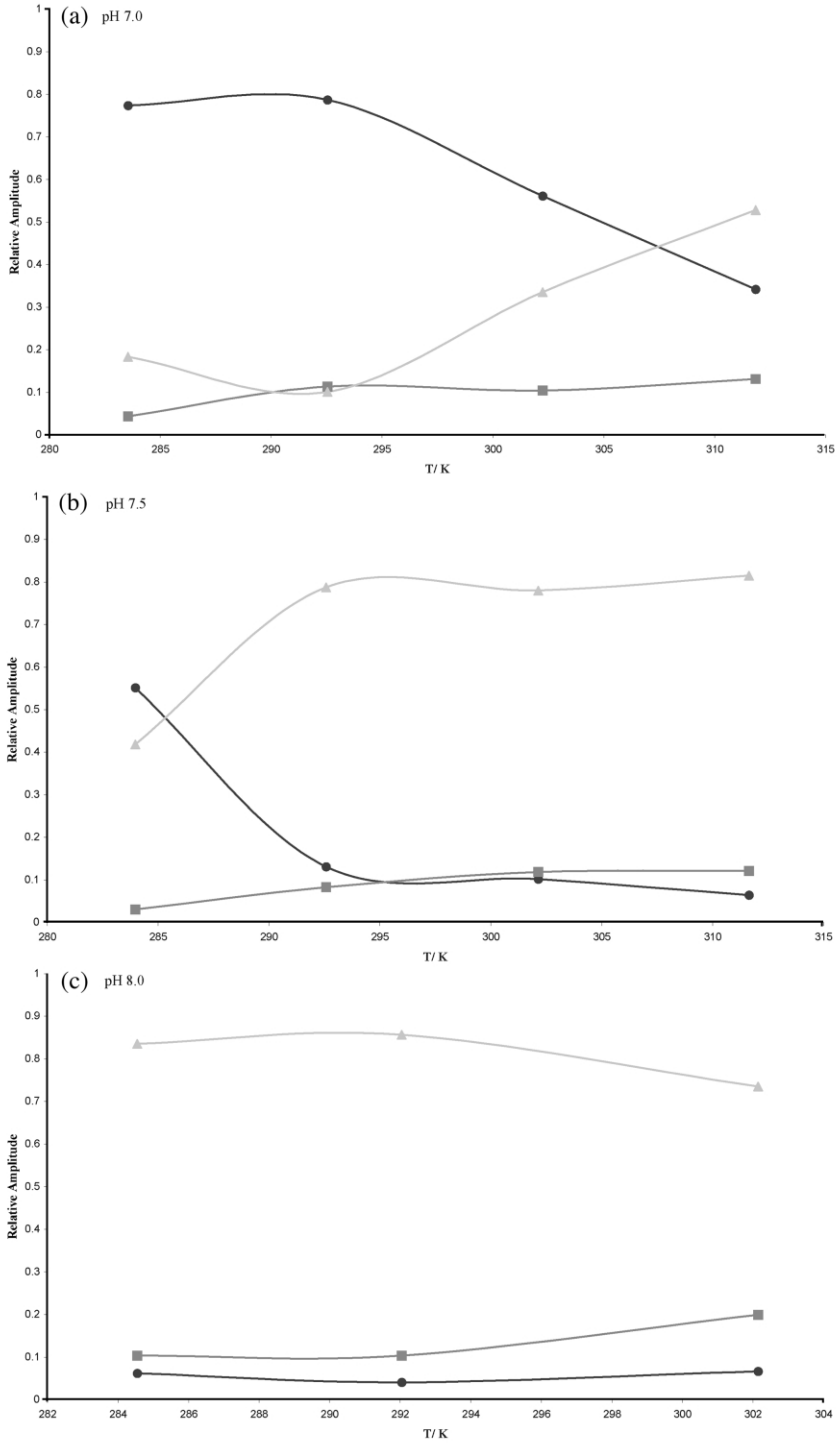

Fig. 4. Relative amplitudes for the three phases of reduction of free $Av2_0$—A_1 (●), A_2 (■), and A_3 (▲) from Eq. (8)—as a function of temperature and pH: (a) pH 7.0; (b) pH 7.5; and (c) pH 8.0.

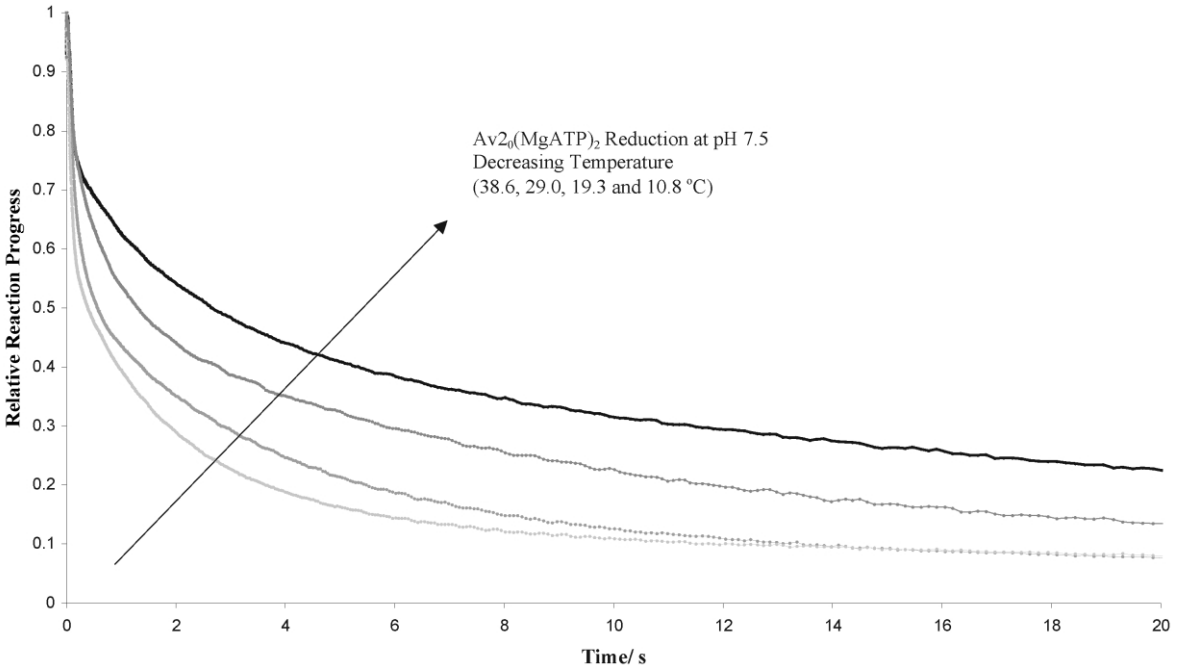

Fig. 5. The reduction of 20 ± 3 μM $Av2_0$ in 4.4 mM ATP and 5.0 mM Mg^{2+} by 0.25 mM DT at 10.8, 19.3, 29.0, and 38.6 °C; and pH held constant at 7.5 in 50 mM inorganic phosphate buffer. The data shown are representative of the temperature effect on $Av2_0(MgATP)_2$ reduction at all pH values studied, and have been modified according to Eq. (11) to facilitate a qualitative comparison.

orous approach in this work is satisfactory since a determination of k_{-DT} vs. temperature has been performed elsewhere [7], and since our results are sufficient to show there is not likely a pH effect on k_{-DT}.

4.2. Reduction of $Av2_0(MgATP)_2$ by DT

Fig. 5 shows representative kinetic traces for the reduction of $Av2_0(MgATP)_2$ as a function of temperature. A striking difference between Figs. 1 and 5 is that the traces in Fig. 1 are encountered from left to right with increasing temperature, while in Fig. 5 traces are encountered from left to right with decreasing temperature. The reason for this difference is that the combined amplitude of phases 1 and 2 with $Av2_0(MgATP)_2$ reduction increases, when the temperature rises from 10 to 40 °C (approx. 65 to 85% at pH 7.0, 55 to 80% at pH 7.5, and 40 to 75% at pH 8.0), while the opposite trend is seen with $Av2_0$ reduction. However, the effects of pH on the amplitudes of phases of $Av2_0(MgATP)_2$ reduction follow the trend seen with $Av2_0$ reduction (compare Figs. 2 and 6). Table 1 summarizes the thermodynamic activation parameters of the different phases of $Av2_0(MgATP)_2$ reduction, and gives constants *a*, *b*, *c* and *d* for use with Eq. (12). Note that only the rate for phase 3 actually demonstrates a pH effect on the rate of reduction, apart from the pH effect on the amplitudes of each phase discussed above.

4.3. Reduction of $Av2_0(MgADP)_2$ by DT

There are three phases of $Av2_0(MgADP)_2$ reduction. The effects of temperature and pH on the reaction can be seen in Figs. 7 and 8. In Fig. 7, the rate of the fast phases of reduction increases with increasing temperature as expected. In addition, the combined amplitude of the two fast phases ($n=1$ and $n=2$) rises until 20 °C, and then falls

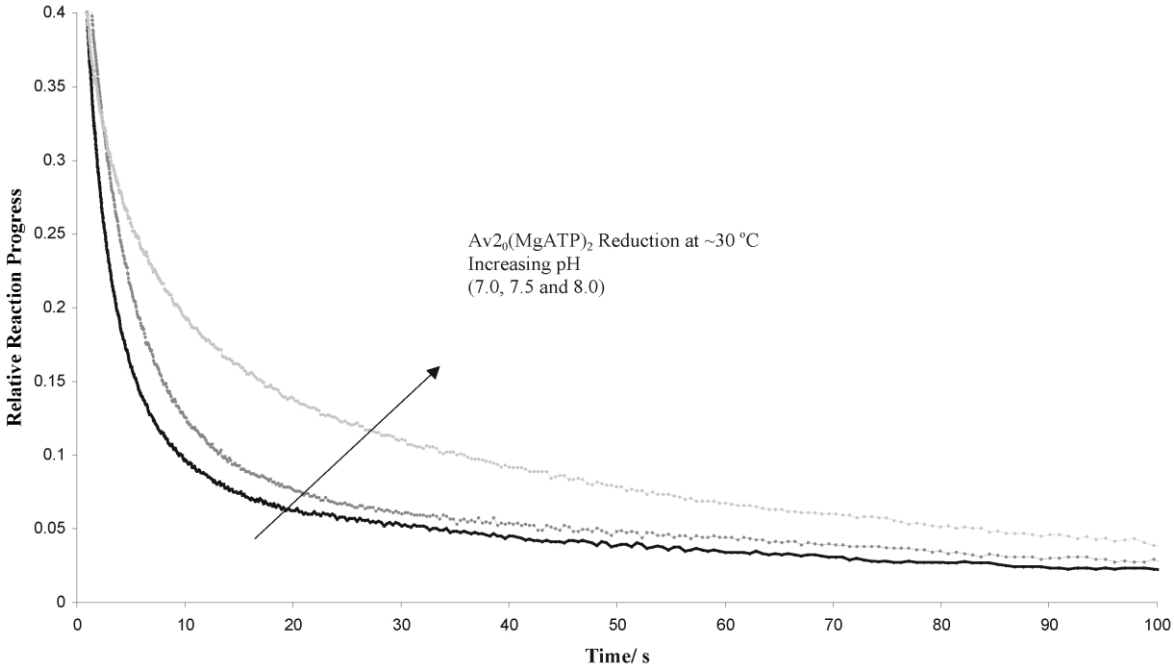

Fig. 6. The reduction of 20 ± 3 μM $Av2_0$ in 4.4 mM ATP and 5.0 mM Mg^{2+} by 0.25 mM DT at pH 7.0, 7.5, and 8.0 in 50 mM inorganic phosphate buffer; and temperature held constant at ~29 °C. The data shown are representative of the pH effect on $Av2_0(MgATP)_2$ reduction at all temperatures studied, and have been modified according to Eq. (11) to facilitate a qualitative comparison.

at higher temperatures. Similarly, the combined amplitude of the two fast phases is maximum at pH 7.5, and diminished at pH 7.0 and 8.0. The fast phases are favored, then, at 20 °C and pH 7.5. While this effect is slight, it is nevertheless consistent over almost the entire range of data in phosphate buffer.

The dominant phase of $Av2_0(MgADP)_2$ reduction is the slower of the two fast reactions ($n=2$). Its amplitude is relatively constant at approximately 86% of the total absorbance change over the range of experimental conditions. Phase 1 accounts for approximately 14% of the absorbance change at all pH values but temperatures less than or equal to 30 °C. At higher temperatures, the contribution from phase 1 is abolished—perhaps because at higher temperatures, the rate of phase 2 overtakes the assumed rate of phase 1 so that the two are indiscernible—and compensated for by phase 3, which is present only to a much smaller extent at lower temperatures.

The thermodynamic activation parameters of the phases of $Av2_0(MgADP)_2$ reduction and constants for determining the rate constants as a function of pH and temperature are summarized in Table 1. It should be noted that we could only detect a pH effect for the dominant phase ($n=2$). Perhaps the minor phases have a pH effect, but as with phase 2 of $Av2_0$ reduction, the low amplitudes of these phases contribute to difficulties in measuring their corresponding rate constants accurately enough to discern a pH effect.

5. Discussion

5.1. Protein activity

The rates of reduction of $Kp2_0$ (45% active) and $Ac2_0$ (65–75% active) with DT have been reported to have four distinct exponential phases [2] [14]. The fast phase was attributed to active protein, while the remaining slower phases did not

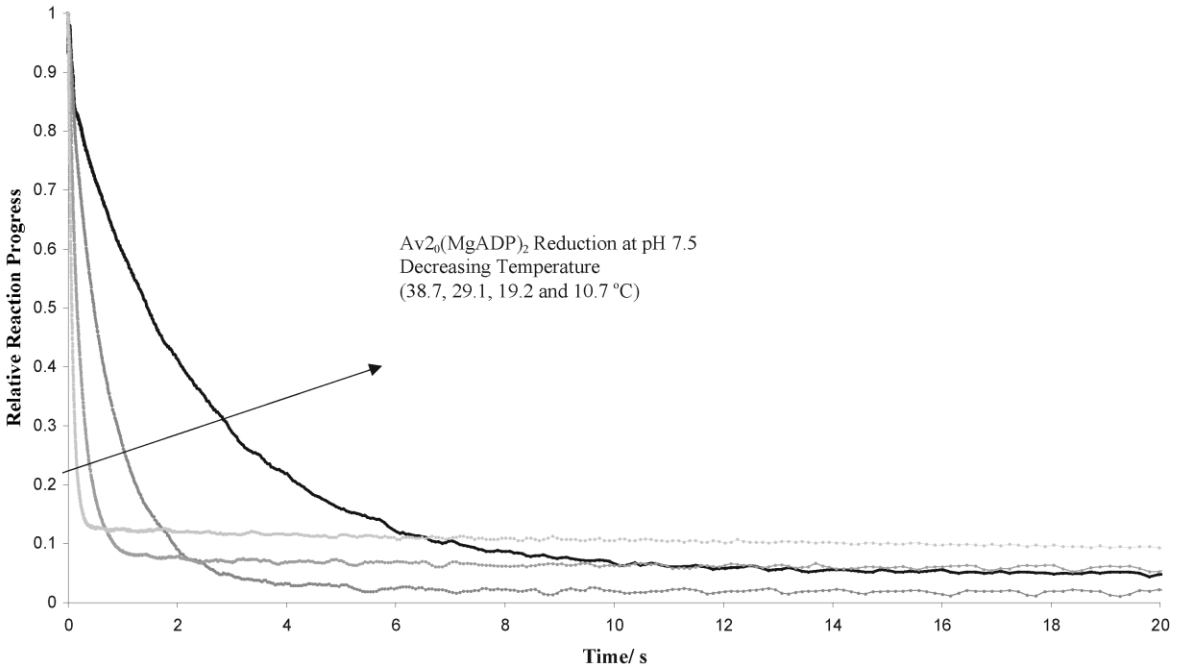

Fig. 7. The reduction of 20 ± 3 μM $Av2_0$ in 4.4 mM ADP and 5.0 mM Mg^{2+} by 0.25 mM DT at 10.7, 19.2, 29.1, and 38.7 °C; and pH held constant at 7.5 in 50 mM inorganic phosphate buffer. The data shown are representative of the temperature effect on $Av2_0(MgADP)_2$ reduction at all pH values studied, and have been modified according to Eq. (11) to facilitate a qualitative comparison.

manifest the characteristic change in EPR signal upon reduction, and were assumed to originate from reduction of O_2-inactivated Fe protein. In the present study, we have observed only three exponential phases of free $Av2_0$ reduction. The question remains whether the two slower phases correspond to active or inactive protein.

Given the extinction coefficients of the reduced and oxidized forms of Av2 [8], the total absorbance changes for our runs accounted for all the Av2 present within the limits of experimental error. This observation suggests that if there were inactive protein present, at least one of two conditions must be true: either the extinction coefficients of the forms of Av2 are not changed by inactivation (whether O_2 inactivation or some other kind); or the amount of inactive protein is small, so that it falls beyond the limits of detection.

The specific activity was measured to be 1800–2000 nmol of H_2 min^{-1} mg^{-1} in standard activity assays [9] before being loaded into the stopped-flow apparatus and after the completion of the kinetic measurements. The activity after the measurements was only up to 10% less than the original activity, which is consistent with the possibility of only a small activity loss upon initial oxidation as reported previously [1]. This observation suggests that, given the highly active nature of Av2 when compared to Fe protein of species other than *A. vinelandii*, the slower phases of $Av2_0$ reduction actually represent active protein. Furthermore the combined amplitude of the fastest reactions for $Av2_0(MgADP)_2$ reduction was as high as 97% of the total absorbance change at pH 7.5 and 20 °C (see Fig. 7). If the slower phases of $Av2_0$ reduction could be attributed to inactive protein, then the same protein should give similar amplitudes for slow reduction of nucleotide-bound forms of protein. In the case of $Av2_0(MgADP)_2$, the average relative amplitude of the slow phase over the entire range of pH and temperature studied was approximately 6% of the total absorbance change, while

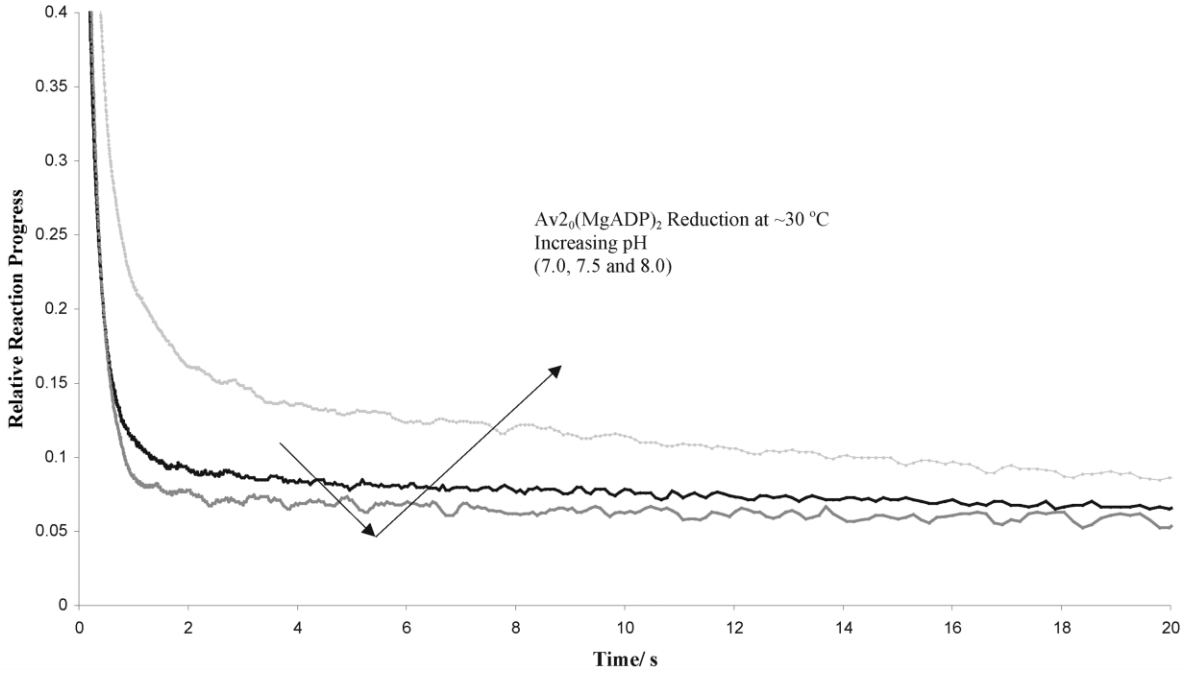

Fig. 8. The reduction of 20 ± 3 μM $Av2_0$ in 4.4 mM ADP and 5.0 mM Mg^{2+} by 0.25 mM DT at pH 7.0, 7.5, and 8.0 in 50 mM inorganic phosphate buffer; and temperature held constant at ~29 °C. The data shown are representative of the pH effect on $Av2_0(MgADP)_2$ reduction at all temperatures studied, except at 10 °C where the peak in amplitude of A_1 is not so obvious. The data have been modified according to Eq. (11) to facilitate a qualitative comparison.

15% of the absorbance change in $Av2_0(MgATP)_2$ reduction could be attributed to the slowest reaction in phosphate buffer. We attribute the slower phases of $Av2_0$ reduction to different conformations of the protein—the relative amounts of which change with pH, temperature, and solution buffer—and not to inactive protein.

A. vinelandii nitrogenase is generally considered to be very active when compared to nitrogenase of other species, but it was determined in one study of the Fe protein cycle that Av2 is only 62% active [15], so it would be of interest to determine whether the slower phases of Av2 reduction are attributable to active protein conformers for each of the variants $Av2_0$, $Av2_0(MgADP)_2$, and $Av2_0(MgATP)_2$. Specifically, one could measure the EPR change that occurs upon Av2 reduction under conditions where such data could be obtained manually as described in this work. However, this is beyond the scope of the present study.

5.2. Populations of different conformers of the Fe protein vary with temperature and pH

While there is undoubtedly a continuum of conformations of Av2 in solution—each with different rates of reduction—there are likely just a few that are important to nitrogenase catalysis. Furthermore, it is likely that if a particular conformation favors reduction of one Av2 species over another, then natural selection would have favored it to dominate the relative absorbance change of Av2 reduction under physiological conditions. Such appears to be the case for $Av2_0(MgADP)_2$ reduction. From Figs. 7 and 8, we noted how there is consistently a peak in the combined amplitude of the two faster phases favoring reduction at pH 7.5 and 20 °C, at which point the fast phases account for 97% of the total absorbance change. With higher resolution of temperature and pH it

should be possible to narrow the exact conditions favoring this reaction.

It has long been thought that $Av2_0(MgADP)_2$ reduction is catalytically relevant [16]. Our data provides supporting evidence for this idea, as the other two possibilities—$Av2_0$ and $Av2_0(MgATP)_2$—only favor rapid reduction at a particular extreme. Specifically, A_1 for $Av2_0$ is highest at pH 7.0 and 10–20 °C (see Fig. 4), while (A_1+A_2) for $Av2_0(MgATP)_2$ is highest at pH 8.0 and 40 °C. Neither of these extremes represents ideal physiological conditions. It may be, however, that reduction of $Av2_0$ and $Av2_0(MgATP)_2$ may be compensatory mechanisms for Fe protein reduction under conditions of physiological stress.

Still, it is important to emphasize that the experimental conditions in this study are not physiologically relevant because dye-oxidized Av2 was used, and it was reduced by a non-physiological reductant. Therefore this study at most only lends supporting evidence to the notion that $Av2_0(MgADP)_2$ reduction is catalytically relevant, but not definitive proof that this is the case.

Ashby et al. proposed that there are different conformers of the $Kp2_0$ protein in both free and MgADP-bound forms [3]. It was determined that these conformers are interchangeable and that the relative populations of each are responsible for Kp2 being only 45% active—where one conformer is catalytically inactive, but is nevertheless reduced rapidly. Furthermore, Miller et al. showed that $Kp2_0(MgADP)_2$ and $Kp2_0(MgATP)_2$ transiently assume the $Kp2_1(MgADP)_2$ and $Kp2_1(MgATP)_2$ conformations, respectively, in the absence of DT [17], though it is not clear whether these conformers correspond to the rapidly reduced but inactive conformers seen by Ashby et al.

It is possible that Av2 has similar conformers, though their activity level may be different than they are for Kp2 since Av2 is much more active. It has been suggested that Av2 has different conformers when bound to MgATP [5], owing to the observation of a double exponential for both the reduction of $Av2_0(MgATP)_2$, as well as the chelation reaction of Fe from the [4Fe–4S] cluster of the MgATP-bound Fe protein [18].

As noted previously, we have observed four exponential phases for the reduction of $Av2_0(MgATP)_2$, while Lanzilotta et al. noted only two exponential phases [5]. There is also a difference of two between the number of exponential phases we report for $Av2_0(MgADP)_2$ reduction. However, with both nucleotides the amplitudes of the slowest phases that we have observed are very small. Our respective protein activities are comparable, so the differences are unlikely to be due to inactive protein. It may be that the kinetic traces of Lanzilotta et al. did not run so long as ours—200 s for $Av2_0(MgADP)_2$ and 500 s for $Av2_0(MgATP)_2$—or that the minimal contribution of the slowest phase was not evaluated. This seems likely because A_2 for $Av2_0(MgADP)_2$ reduction is only 3% of the total absorbance change at pH 7.5 and 20 °C, very close to the experimental conditions of Lanzilotta et al., though not in the same buffer. Furthermore, it has been suggested that if slower phases are observed, they may be difficult to measure if their amplitude is small [3]. As this is the first study to investigate these reactions over wide ranges of temperature and pH—under conditions where the amplitudes of slower phases can be more pronounced—it may be that this is the first time the slower phases have been seen as relevant.

5.3. An accelerated phase of $Av2_0(MgANP)_2$ reduction

Interestingly, our analysis of both $Av2_0(MgATP)_2$ and $Av2_0(MgADP)_2$, reduction revealed a previously uncharacterized faster phase in addition to the previously uncharacterized slower phase described above. As this phase is also a minor contributor to the total absorbance change, it may have been previously attributed to an anomaly of instrumentation, or missed entirely if the time resolution were poor for early *t*. Only when this very fast phase was fit as its own phase were we able to reconcile apparent differences between rate constants from runs of high time resolution to runs of low time resolution.

The rates of phase 1 for $Av2_0$ and $Av2_0(MgADP)_2$ reduction are remarkably similar,

as determined by a comparison of rate constants in Table 1 and Eq. (12). One may postulate that there is a small population of Av2 in a sample of $Av2(MgADP)_2$ that is unbound by nucleotide, and so is reduced at the rate of phase 1 for $Av2_0$, since that is the dominant phase for $Av2_0$ reduction. However, MgADP binds Av2 more tightly than does MgATP [19]. If there is free $Av2_0$ in a sample of $Av2_0(MgADP)_2$, then there should be more of it in a sample of $Av2_0(MgATP)_2$ at the same nucleotide concentrations. If this were the case, the fastest phase for both $Av2_0(MgADP)_2$ and $Av2_0(MgATP)_2$ reduction would have the same rate, but a larger amplitude in the sample of $Av2_0(MgATP)_2$. This is not observed. Rather, the fastest rate of $Av2_0(MgATP)_2$ reduction is much slower than the corresponding phase of $Av2_0(MgADP)_2$ reduction. However, it is interesting that the amplitude of the fastest phase of reduction is more prominent in $Av2_0(MgATP)_2$ than in $Av2_0(MgADP)_2$, perhaps corresponding to a larger relative population of $Av2_0$MgATP in a sample of $Av2_0(MgATP)_2$ than $Av2_0$MgADP in a sample of $Av2_0(MgADP)_2$. Indeed, it is more difficult to rule out $Av2_0$MgATP and $Av2_0$MgADP as candidates for phase-1 reductions than it is to rule out $Av2_0$.

One way to confirm or disprove the presence of $Av2_0$MgANP ($Av2_0$MgATP or $Av2_0$MgADP) is to vary the concentration of nucleotides and observe the effect on the amplitude of the phase-1 reductions. If $Av2_0$MgANP reduction were responsible for phase-1 reactions, then the phase-1 amplitudes would increase at lower nucleotide concentrations and diminish at higher nucleotide concentrations. However, at our concentrations of 4.4 mM MgANP, there should be approximately 99.7% $Av2_0(MgANP)_2$, 0.3% $Av2_0$MgANP, and a very small quantity of free $Av2_0$, based on the most recently determined values of dissociation constants K_{d2} and K_{d1} of MgANP from $Av2_0(MgANP)_2$ and $Av2_0$MgANP. [20] Unfortunately, there is considerable disagreement in the literature about the measurements of apparent K_d for the Fe protein and nucleotides, and earlier estimates of the apparent K_d for $Av2_0(MgANP)_2$ [19] predict a much more significant population of free $Av2_0$—9.1% of the total Fe Protein at our concentration of MgATP, or 1.35% in our samples with MgADP. As mentioned above, there is not a significant quantity of free $Av2_0$ in our nucleotide-containing samples, so values for an apparent K_d are unlikely to be applicable to our analysis. An area of ongoing research in our lab is to vary nucleotide concentrations to determine if phase 1 for $Av2_0(MgATP)_2$ and $Av2_0(MgADP)_2$ reduction can be attributed to $Av2_0$MgANP species. If this is the case, it should be possible to adjust nucleotide concentrations so that there are sufficient populations of $Av2_0$, $Av2_0$MgANP, and $Av2_0(MgANP)_2$ to measure K_{d1} and K_{d2} for MgANP in the stopped-flow apparatus as a function of temperature and pH.

If this line of investigation proves unfruitful, it may be that the faster phase of $Av2_0(MgANP)_2$ reduction can be attributable to the inactive, rapidly-reduced conformer proposed by Ashby et al. for $Kp2_0$ [3].

5.4. Buffer effects on Fe protein reduction

Depending on the buffer used to perform Fe protein reduction reactions, there is a change in the amplitudes of the different phases. Fig. 9 illustrates this buffer effect for $Av2_0$ reduction. For the same conditions of pH 7.5 and temperature 24.0 °C, the fast phase is favored in TES buffer. HEPES also heavily favors the fast phase (data not shown). To a lesser extent, the fast phase is favored in Tris buffer; and in phosphate buffer, it is favored the least of any buffer tested.

While the fast phase is not favored in phosphate buffer as much as it is in other buffers, the reverse is true for the reduction of both $Av2_0(MgATP)_2$ (Fig. 10) and $Av2_0(MgADP)_2$ (Fig. 11). In each case, phosphate favors rapid reduction. The next best buffer is TES, then HEPES (data not shown for $Av2_0(MgATP)_2$ reduction), and then Tris.

Having performed Fe protein reduction reactions in buffers where certain phases are more important than in others, we have been able to measure certain rate constants more accurately than would have been possible from measurements in a single buffer alone. In particular, phase 3 of $Av2_0$ reduction was an important phase in phosphate buffer, while generally undetectable in each of the other

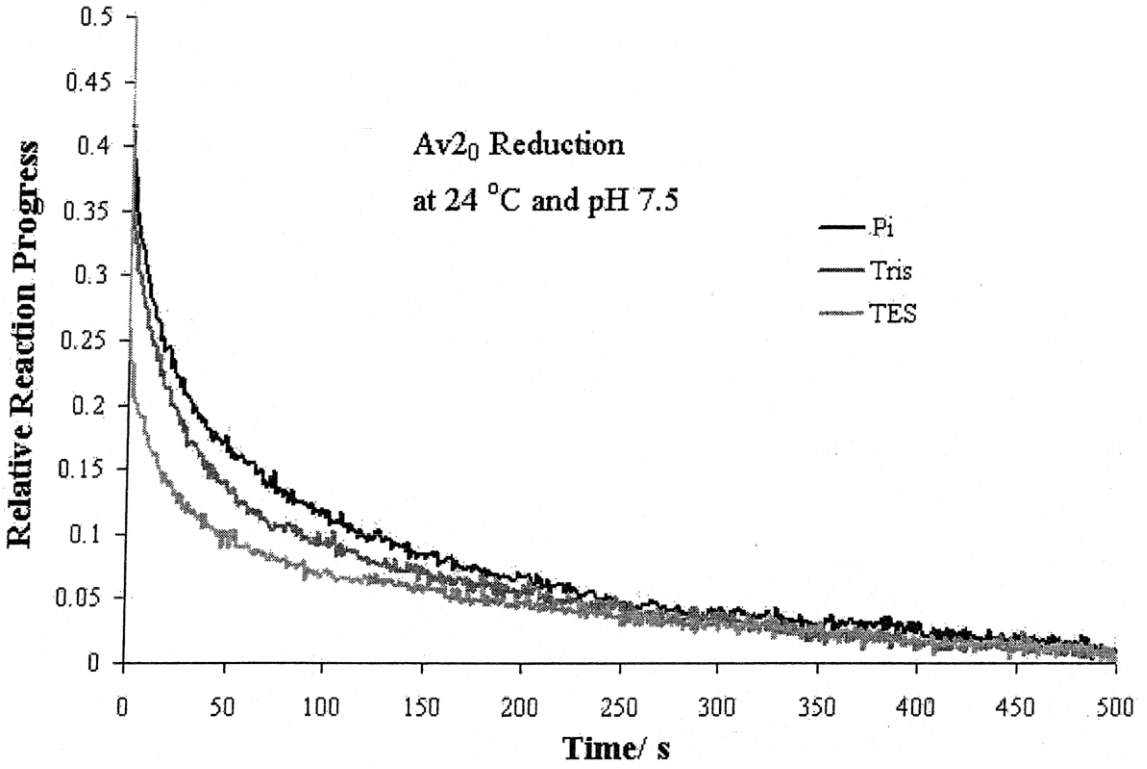

Fig. 9. The reduction of 20 ± 3 μM, free $Av2_0$ by 0.25 mM DT at 24 °C and pH 7.5 in 50 mM inorganic phosphate, Tris and TES buffers. The data shown are representative of the buffer effect on $Av2_0$ reduction over the range of experimental conditions in this work, and have been modified according to Eq. (11) to facilitate a qualitative comparison.

buffers tested; and phase 4 of $Av2_0(MgATP)_2$ reduction, while minor in phosphate buffer, is a major contributor to the overall reaction in Tris buffer. It should be noted that in Figs. 10 and 11 the data are compared over the same time scale, with poor resolution at early *t*, essentially truncating off the fast phase-1 reactions, so the comparison is for phases of $n > 2$.

An important observation with experiments done in different buffers is that the general trends of how the amplitudes of the different phases of a reaction change with temperature and pH are the same as they are in inorganic phosphate buffer. In addition, the corresponding rates are unchanged with the buffer.

5.5. Effects of nucleotides on the reduction of $Av2_0$ for pH 7–8 and 10–40 °C

It has been observed previously that ATP does not affect the rate of Ac2 reduction when compared to free Ac2 [1]. On the contrary, Av2 showed a marked drop in the rate of Fe protein reduction upon addition of MgADP, and an even greater drop in the rate in the presence of MgATP [5]. The present work supports this view of Av2 reduction. It may be that incubation of protein with MgATP prior to protein reduction is responsible for the apparent difference in ATP inhibition being present in Av2 reduction (incubated) and absent in Ac2 reduction (not incubated). Even so, multiple phases of the reaction must be considered.

Given the constants in Table 1, one may actually calculate a rate for phase-1 $Av2_0(MgADP)_2$ reduction comparable to phase-1 $Av2_0$ reduction. However, there is considerable error in the measurement of phase-1 $Av2_0(MgADP)_2$ reduction. It is more reasonable to assume that a more accurate measurement of phase-1 $Av2_0(MgADP)_2$ reduction will

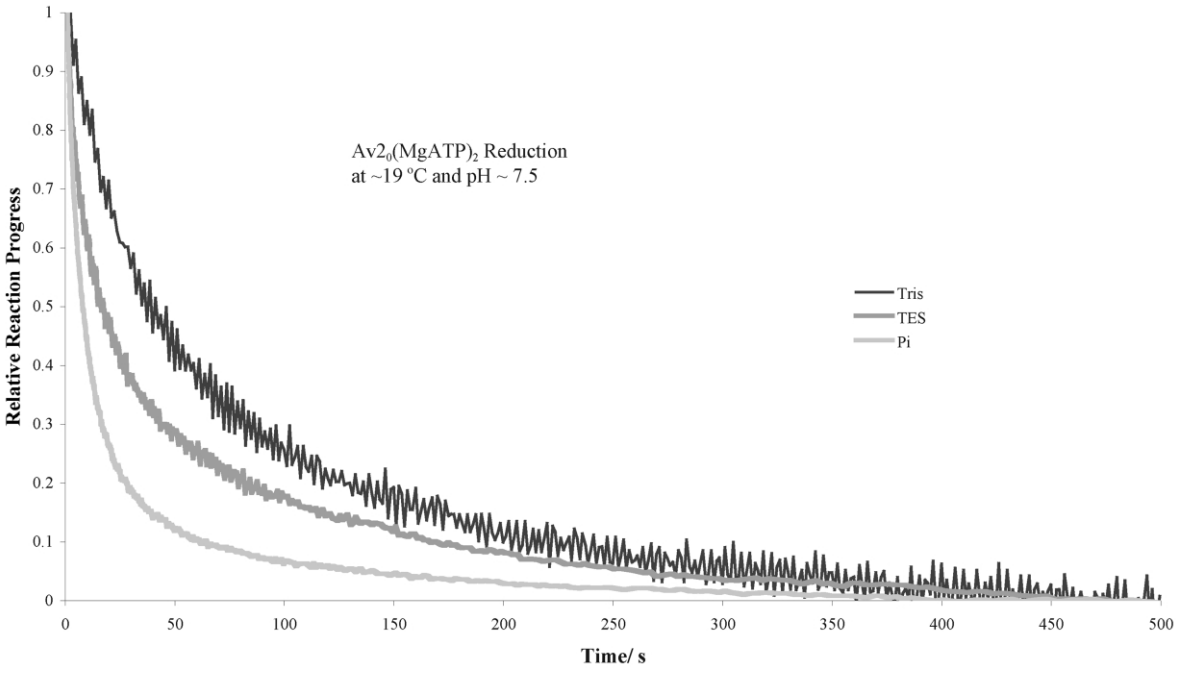

Fig. 10. The reduction of 20 ± 3 μM $Av2_0$ in 4.4 mM ATP and 5.0 mM Mg^{2+} by 0.25 mM DT at ~19.3 °C and pH ~7.54 in 50 mM inorganic phosphate, Tris and TES buffers. The data shown are representative of the buffer effect on $Av2_0(MgATP)_2$ reduction over the range of experimental conditions in this work, and have been modified according to Eq. (11) to facilitate a qualitative comparison, particularly to compensate for time resolution differences at early *t*.

yield results more in line with the overall effect of nucleotides shown in Fig. 12. Furthermore, the contribution from phase-1 $Av2_0(MgADP)_2$ reduction is very minor compared to the dominant phase 2. Fig. 12 shows that at pH 7.5 and ~19.3 °C $Av2_0$ reduction is much faster for early *t*, but because a much slower phase 3 is responsible for much of the overall reaction, $Av2_0(MgADP)_2$ reduction overtakes it at approximately 0.6 s. Phase-1 $Av2_0(MgATP)_2$ reduction is faster than phase-2 $Av2_0(MgADP)_2$ reduction for all pH values and all temperatures less than or equal to ~35 °C, but it is from 4 to 35 times slower than phase-1 $Av2_0(MgADP)_2$ reduction over 10–40 °C. Since the amplitude of phase-1 $Av2_0(MgATP)_2$ reduction is generally larger than the amplitude of phase-1 $Av2_0(MgADP)_2$ reduction, a progress curve for $Av2_0(MgATP)_2$ reduction may start slightly slower than one for $Av2_0(MgADP)_2$ reduction, but may overtake $Av2_0(MgADP)_2$ reduction in overall reaction progress for a very short time, then falling behind as slower phases of $Av2_0(MgATP)_2$ reduction begin to take over. Clearly, a comparison of rate constants of the different phases of Fe protein reduction is insufficient to assess which overall reaction ($Av2_0$, $Av2_0(MgATP)_2$ or $Av2_0(MgADP)_2$ reduction) will proceed more quickly overall. An understanding of how the amplitudes of each phase vary with temperature and pH is also important.

5.6. Survey of literature values for k_r

In light of novel observations in this work, it is important to assess in what ways our work coincides with previously published results. Table 2 shows the rate constants of reduction, k_r, for various forms of the Fe protein from different organisms. Values derived from the literature were either determined by the original authors, or calculated from given values of k_{obs} and [DT], where k_{obs} equals $k_r K_{DT}^{1/2} [DT]^{1/2}$. Values from this work

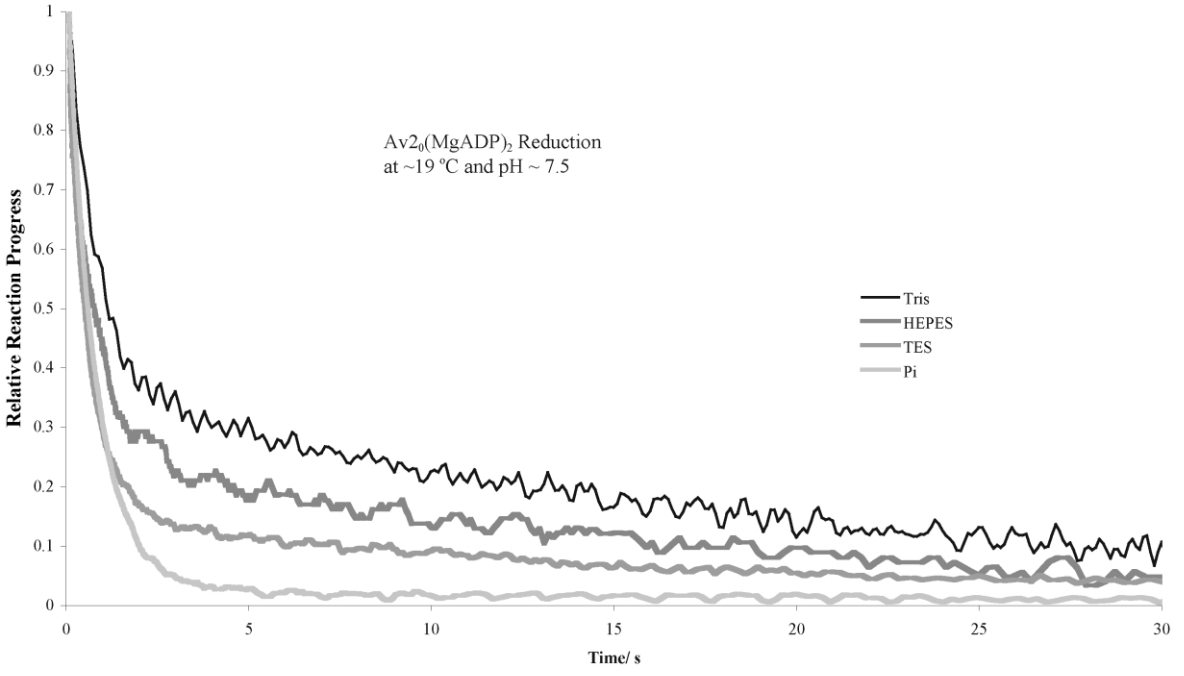

Fig. 11. The reduction of 20 ± 3 μM $Av2_0$ in 4.4 mM ADP and 5.0 mM Mg^{2+} by 0.25 mM DT at ~19.2 °C and pH ~7.55 in 50 mM inorganic phosphate, TES, HEPES and Tris buffers. The data shown are representative of the buffer effect on $Av2_0(MgADP)_2$ reduction over the range of experimental conditions in this work, and have been modified according to Eq. (11) to facilitate a qualitative comparison, particularly to compensate for time resolution differences at early *t*.

were derived from the constants in Table 1 with Eq. (12) at pH 7.4 and 23 °C. The value of $K_{DT} =$ 1.46 nM was used, as determined previously at pH 7.4 and 23 °C [16]. Table 2 does not include some of the phases of Fe protein reduction of this study, only the dominant ones that can be readily compared with literature results.

One major discrepancy in the literature is shown in Table 2. For $Ac2_0$ and $Kp2_0$, MgADP slows down Fe protein reduction while MgATP does not [1,14]. However, this work and other recent studies [6,21] show that MgATP inhibits $Av2_0$ reduction even more than MgADP, particularly when taking into account the relative amplitudes of the slower phases for the reduction of Fe protein bound to MgATP (see Fig. 12). It may be that the effects of MgATP on Fe protein reduction are confined to $Av2_0$, though if this were the case, it would be curious that there is such agreement in the literature on the rate of reduction of free Fe protein and Fe protein bound to MgADP, as in Table 2. Our results coincide well with previous work on $Av2_0$.

5.7. Activation parameters of Fe protein reduction

In an attempt to understand the differences between the respective phases of Fe protein reduction, we calculated the activation parameters (energies, enthalpies, and entropies) for the component phases of the overall reduction processes, as summarized in Table 1. With free $Av2_0$, the slower phases have progressively lower activation energies and enthalpies, as well as more negative activation entropies. The exact reverse is seen with $Av2_0(MgATP)_2$ reduction. $Av2_0(MgADP)_2$ reduction is mixed, with higher activation energy, enthalpy and entropy going from phase 1 to phase 2, but then a drop in these parameters going from phase 2 to phase 3.

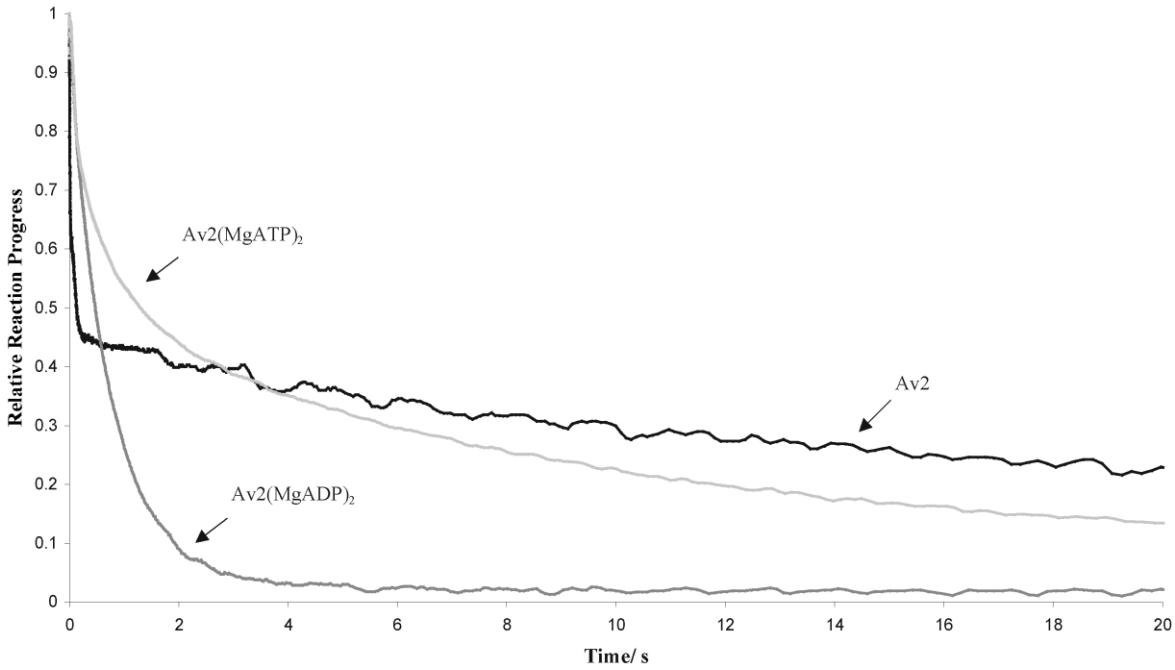

Fig. 12. Nucleotides (4.4 mM ANP, 5 mM Mg) slow the reduction of 20 ± 3 μM $Av2_0$ by 0.25 mM DT at pH 7.5 and ~19.3 °C in inorganic phosphate buffer. The data shown are representative of the effect of nucleotides at all temperatures and pH values studied, and have been modified according to Eq. (11) to facilitate a qualitative comparison.

5.8. The break in the Arrhenius plot for activity is likely a property of the nitrogenase protein–protein complex

A break has been observed in the Arrhenius plot of both nitrogenase activity and primary electron transfer from the Fe protein to the MoFe protein [22–27]. The cause of this break is believed to be a conformational change in one or both components of nitrogenase, leading to a change in the affinity of the Fe protein–MoFe protein complex [23–26,28]. It has been suggested that the MoFe

Table 2
Comparison of rate constants for Fe protein reduction at ~23 °C and pH ~7.4. Only certain phases from this work are represented: phase 1 for $Av2_0$; phases 2 and 3 for $Av2_0(MgATP)_2$; and phase 2 for $Av2_0(MgADP)_2$

	Organism	T/°C, pH	$k_{r,\ fast}/(M^{-1}\ s^{-1})$	$k_{r,\ slow}/(M^{-1}\ s^{-1})$	Refs.
Free	Kp	23, 7.4	$>1\times10^8$		[3]
	Ac	23, 7.4	$>1\times10^8$		[2]
	Av	23, 7.4	1.7×10^8		[5]
			1.9×10^8		This Work
MgATP	Ac	23, 7.4	$\sim1\times10^8$		[1]
	Av	23, 7.4	1.9×10^6	1.3×10^5	[5]
			1.2×10^6	1.5×10^5	This Work
	Kp	23, 7.4	3×10^6		[3,16]
	Ac	23, 7.4	2.9×10^6		[1]
		23, 7.2	4.7×10^6		[4]
MgADP	Av	23, 7.4	3.7×10^6		[5]
		22, 7.4	4.5×10^6		[6]
		23, 7.4	3.5×10^6		This Work
		20, 7.4	3×10^6		[29]
		20, 7.4	2.4×10^6		This Work

protein is a noteworthy candidate for this proposed temperature-dependent conformational change, as its interaction with CO experiences a sharp increase above 15 °C in nitrogenase from *Klebsiella pneumoniae* [23].

Still, it has been proposed that a change in both component proteins may be required to explain breaks in both electron transfer and ATP hydrolysis [25]. It is likely that such a conformational change in the Fe protein is inherent in the formation of the protein–protein complex. However unlikely, it may also be inherent in the Fe protein itself. If a significant temperature-dependent conformational change were inherent in the individual protein components of nitrogenase, and not just in the nitrogenase complex, then we would expect it to influence a series of steps in the catalytic cycle, such as Fe protein reduction. However, we have not observed any break in the Arrhenius plots of Fe protein reduction in this study. Still, relative contributions of different phases of reduction are also important. Since phase-2 reduction of $Av2_0(MgADP)_2$ is likely the catalytically relevant reaction, any argument for the importance of relative amplitude must address this phase. We have noted that it is dominant over the range of 10–40 °C and pH 7–8, and the effects of temperature and pH on its amplitude are minimal. Therefore, the break in the Arrhenius plots for activity and electron transfer are likely attributable to the MoFe protein and/or the nitrogenase complex, and not some property inherent in the Fe protein alone.

Acknowledgments

This research was supported by the College of Mathematics and Physical Sciences at Brigham Young University.

References

[1] M.G. Yates, R.N.F. Thorneley, D.J. Lowe, Nitrogenase of *Azotobacter chroococcum*: inhibition by ADP of the reduction of oxidized Fe protein by sodium dithionite, FEBS Lett. 60 (1975) 89.

[2] R.N.F. Thorneley, M.G. Yates, D.J. Lowe, Nitrogenase of *Azotobacter chroococcum* kinetics of the reduction of oxidized iron protein by sodium dithionite, Biochem. J. 155 (1976) 137.

[3] G.A. Ashby, R.N.F. Thorneley, Nitrogenase of *Klebsiella pneumoniae*. Kinetic studies on the iron protein involving reduction by sodium dithionite, the binding of magnesium ADP and a conformation change that alters the reactivity of the iron–sulfur (4Fe–4S) center, Biochem. J. 246 (1987) 455.

[4] J. Bergstrom, R.R. Eady, R.N. Thorneley, The Vanadium-and Molybdenum-containing nitrogenases of *Azotobacter chroococcum*. Comparison of mid-point potentials and kinetics of reduction by sodium dithionite of the iron proteins with bound magnesium adenosine 5′-Diphosphate, Biochem. J. 251 (1988) 165.

[5] W.N. Lanzilotta, K. Fisher, L.C. Seefeldt, Evidence for electron transfer from the nitrogenase iron protein to the molybdenum-iron protein without MgATP hydrolysis: Characterization of a tight protein–protein complex, Biochemistry 35 (1996) 7188.

[6] J. Christiansen, J. Goodwin Paul, N. Lanzilotta William, C. Seefeldt Lance, R. Dean Dennis, Catalytic and biophysical properties of a nitrogenase apo-MoFe protein produced by a nifB-deletion mutant of *Azotobacter vinelandii*, Biochemistry 37 (1998) 12611.

[7] D.O. Lambeth, G. Palmer, The kinetics and mechanism of reduction of electron transfer proteins and other compounds of biological interest by dithionite, J. Biol. Chem. 248 (1973) 6095.

[8] D. Thiriot, Department of Chemistry and Biochemistry, Brigham Young University, Provo 1995, p. 58.

[9] B.K. Burgess, D.B. Jacobs, E.I. Stiefel, Large scale purification of high activity *Azotobacter vinelandii* nitrogenase, Biochim. Biophys. Acta 614 (1980) 196.

[10] G.L. Anderson, J.B. Howard, Reactions with the oxidized iron protein of *Azotobacter vinelandii* nitrogenase formation of a 2 iron center, Biochemistry 23 (1984) 2118.

[11] G.D. Watt, Z.C. Wang, Further redox reactions of metal clusters in the molybdenum-iron protein of *Azotobacter vinelandii* nitrogenase, Biochemistry 25 (1986) 5196.

[12] N.E. Good, G.D. Winget, W. Winter, T.N. Connolly, S. Izawa, R.M. Singh, Hydrogen ion buffers for biological research, Biochemistry 5 (1966) 467.

[13] D.C. Harris, Nonlinear least squares curve fitting with microsoft excel solver, J. Chem. Educ. 75 (1998) 119.

[14] R.N. Thorneley, Nitrogenase of *Klebsiella pneumoniae*. A stopped-flow study of magnesium–adenosine triphosphate–induced electron transfer between the compeonent proteins, Biochem. J. 145 (1975) 391.

[15] M.G. Duyvis, H. Wassink, H. Haaker, Pre-steady-state kinetics of nitrogenase from *Azotobacter vinelandii*. Evidence for an ATP-induced conformational change of the nitrogenase complex as part of the reaction mechanism, J. Biol. Chem. 271 (1996) 29632.

[16] R.N.F. Thorneley, D.J. Lowe, Kinetics and mechanism of the nitrogenase enzyme system, in: T. Spiro (Ed.), Molybdenum Enzymes, 1, Wiley-Interscience, New York, 1985, p. 221.

[17] R.W. Miller, R.R. Eady, C. Gormal, S.A. Fairhurst, B.E. Smith, Nucleotide binding by the nitrogenase Fe protein: A 31P NMR study of ADP and ATP interactions with

the Fe protein of *Klebsiella pneumoniae*, Biochem. J. 334 (1998) 601.
[18] T.L. Deits, J.B. Howard, Kinetics of magnesium ATP-dependent iron chelation from the iron-protein of the *Azotobacter vinelandii* nitrogenase complex evidence for two states, J. Biol. Chem. 264 (1989) 6619.
[19] B.K. Burgess, D.J. Lowe, Mechanism of molybdenum nitrogenase, Chem. Rev. 96 (1996) 2983.
[20] W.N. Lanzilotta, V.D. Parker, L.C. Seefeldt, Thermodynamics of nucleotide interactions with the *Azotobacter vinelandii* nitrogenase iron protein, Biochim. Biophys. Acta 1429 (1999) 411.
[21] W.N. Lanzilotta, L.C. Seefeldt, Electron transfer from the nitrogenase iron protein to the (8Fe-(7-8)S) clusters of the molybdenum-iron protein, Biochemistry 35 (1996) 16770.
[22] R.C. Burns, The nitrogenase system from *Azotobacter*: activation energy and divalent cation requirement, Biochim. Biophys. Acta 171 (1969) 253.
[23] R.N.F. Thorneley, R.R. Eady, M.G. Yates, Nitrogenases of *Klebsiella pneumoniae* and *Azotobacter chroococcum*. Complex formation between the component proteins, Biochim. Biophys. Acta 403 (1975) 269.
[24] G.D. Watt, A. Burns, Kinetics of dithionite ion utilization and ATP hydrolysis for reactions catalyzed by the nitrogenase complex from *Azotobacter vinelandii*, Biochemistry 16 (1977) 264.
[25] F. Ceuterick, J. Peeters, K. Heremans, H. de Smedt, H. Olbrechts, Effect of high pressure, detergents and phospolipase on the break in the Arrhenius plot of *Azotobacter* nitrogenase, Eur. J. Biochem. 87 (1978) 401.
[26] R.E. Mensink, H. Haaker, Temperature effects on the magnesium ATP-Induced electron transfer between the nitrogenase proteins from *Azotobacter vinelandii*, Eur. J. Biochem. 208 (1992) 295.
[27] W.N. Lanzilotta, V.D. Parker, L.C. Seefeldt, Electron transfer in nitrogenase analyzed by Marcus theory: Evidence for gating by MgATP, Biochemistry 37 (1998) 399.
[28] G.D. Watt, W.A. Bulen, A. Burns, K.L. Hadfield, Stoichiometry, ATP/2e values, and energy requirements for reactions catalyzed by nitrogenase from *Azotobacter vinelandii*, Biochemistry 14 (1975) 4266.
[29] M.G. Duyvis, H. Wassink, H. Haaker, Nitrogenase of *Azotobacter vinelandii*: kinteic analysis of the Fe protein redox cycle, Biochemistry 37 (1998) 17345.